Gas phase studies of Na diffusion in He and Ar and kinetics of Na+Cl2 and Na+SF6

Carol L. Talcott, Joel W. Ager, and Carleton J. Howard

Citation: J. Chem. Phys. **84**, 6161 (1986); doi: 10.1063/1.450757
View online: http://dx.doi.org/10.1063/1.450757
View Table of Contents: http://jcp.aip.org/resource/1/JCPSA6/v84/i11
Published by the American Institute of Physics.

Gas phase studies of Na diffusion in He and Ar and kinetics of Na + Cl_2 and Na + SF_6

Carol L. Talcott, Joel W. Ager III, and Carleton J. Howard[a)]
Aeronomy Laboratory, National Oceanic and Atmospheric Administration, Boulder, Colorado 80303 and Department of Chemistry and Biochemistry of the University of Colorado and Cooperative Institute for Research in Environmental Sciences, Boulder, Colorado 80303

(Received 26 December 1985; accepted 1 January 1986)

A fast flow reactor, using an oven source and resonant fluorescence detection, was built to study the kinetics of sodium atoms in the gas phase. The rate coefficients for Na + Cl_2 and Na + SF_6 are $(7.80 \pm 1.6) \times 10^{-10}$ and $(1.17 \pm 0.2) \times 10^{-12}$ cm^3 molecule^{-1} s^{-1}, respectively. Since collisions with the wall remove sodium with approximately unit efficiency, gaseous diffusion coefficients of sodium in the carrier gas can be measured. $D_{Na,He} = 325 \pm 33$ cm^2 Torr s^{-1} at 290 K and $D_{Na,Ar} = 140 \pm 14$ cm^2 Torr s^{-1} at 281 K. The experimental results are compared with previous studies and simple theoretical models.

I. INTRODUCTION

The existence in the Earth's atmosphere of a layer of sodium atoms centered at about 90 km has been known for about 50 years. In 1929 Slipher[1] observed emissions near 590 nm in the night sky. In 1938 Cabannes *et al.*[2] showed the emission to be the Na D line doublet, ($3\,^2P_{1/2,3/2}$) $\rightarrow$ ($3\,^2S_{1/2}$), and correctly suggested meteor ablation as the source. Shortly afterwards Chapman[3] proposed a mechanism for the nighttime emission

$$\mathrm{Na} + \mathrm{O_3} \rightarrow \mathrm{NaO} + \mathrm{O_2}\,, \tag{1}$$

$$\mathrm{NaO} + \mathrm{O} \rightarrow \mathrm{Na}(^2P) + \mathrm{O_2}\,, \tag{2}$$

$$\mathrm{Na}(^2P) \rightarrow \mathrm{Na}(^2S) + h\nu(590\ \mathrm{nm})\,. \tag{3}$$

Several groups[4,5] found enhancements of D line radiation at twilight due to fluorescence of the sodium layer with the sun as the source. Cabannes *et al.*[2] used this method and estimated the height of the layer to be 130 km. Modern methods including lidar,[6–8] rocket borne photometry,[9,10] and observation of the dayglow[11] have found a thin ($\sim$5 km) layer of sodium atoms having a maximum density of a few thousand atom cm^{-3} at 90 $\pm$ 5 km. Meteors are now firmly established as the source.[12,13]

Interest in the stratospheric chemistry of sodium compounds was stimulated by the proposal of Ferguson[14] that an ion of mass 42 $\pm$ 2 amu and its hydrates detected at 37 km by Arnold and co-workers[15,16] was $NaOH_2^+(H_2O)_n \times (NaOH)_m$, where $n = 0$–4 and $m = 0$–2. Liu and Reid[17] modeled the stratospheric chemistry of sodium species and predicted that NaOH would be the major sodium compound below 90 km. Murad, Swider, and Benson[18] proposed that sodium compounds could affect the stratospheric chemistry of chlorine through the formation of NaCl:

$$\mathrm{NaOH} + \mathrm{Cl} \rightarrow \mathrm{NaCl} + \mathrm{OH}\,, \tag{4}$$

$$\mathrm{NaOH} + \mathrm{ClO} \rightarrow \mathrm{NaCl} + \mathrm{HO_2}\,, \tag{5}$$

$$\mathrm{NaOH} + \mathrm{HCl} \rightarrow \mathrm{NaCl} + \mathrm{H_2O}\,, \tag{6}$$

$$\mathrm{NaHCO_3} + \mathrm{HCl} \rightarrow \mathrm{NaCl} + (\mathrm{H_2CO_3}\ \text{or}\ \mathrm{H_2O} + \mathrm{CO_2})\,. \tag{7}$$

They assumed that NaCl would be a stable repository for free chlorine and concluded that these reactions could decrease the catalytic destruction of O_3 by Cl and ClO. Rowland and Rodgers[19] pointed out that NaCl is photolyzed by ultraviolet radiation present in the stratosphere and proposed the following:

$$\mathrm{NaCl} + h\nu(\lambda < 295\ \mathrm{nm}) \rightarrow \mathrm{Na} + \mathrm{Cl}\,. \tag{8}$$

Since HCl is an unreactive reservoir for Cl atoms, reactions (6), (7), and (8) would act to convert inactive chlorine to free chlorine and thus increase the amount of O_3 depletion by stratospheric chlorine. Recently Lamb and Benson[20] have speculated that the NaOH and NaCl will polymerize before descending to the altitude of the ozone layer. Ironically the ions observed by Arnold and co-workers[15,16] were later shown[21] to be mass 41 amu and probably hydrated positive ions of acetonitrile.[22]

Although the study of sodium kinetics is not a new field, the modeling studies mentioned previously had to proceed without experimental information about the relevant atmospheric reactions of Na compounds. Rate constants for the reactions of sodium atoms and dimers with halogenated species, O_2, NO_2, and many other compounds were measured using the diffusion flame technique pioneered in the 1930's by Polanyi and co-workers.[23–27] Magee[28] developed the electron jump or harpoon model to explain the large reaction cross sections found in many reactions between metal vapors and electronegative compounds. In the 1960's the dynamics of many alkali atom + halogen molecule reactions (although apparently not Na + Cl_2) were studied in molecular beams. This work to 1971 was reviewed by Kinsey.[29] Hynes *et al.*[30] have published a thorough discussion of Na flame work. The rate constant of Na + O_2 + M has been measured recently by LIF in a flame by Hynes *et al.*,[30] by flash photolysis-resonant absorption by Husain and co-workers,[31,32] and by LIF in a fast flow reactor by Silver *et al.*[33] In one of the most interesting developments in Na chemistry, the rate constant of reaction (6) was recently found to be fast, 3×10^{-10} cm^3 molecule^{-1} s^{-1}, in a flow tube study by Silver *et al.*[34]

The discharge flow techniques has been successfully used to measure the rate constants of many gas phase reac-

a) Author to whom correspondence should be addressed.

 0021-9606/86/116161-09$02.10

tions. A variation of this technique was used here to quantitatively study the kinetics of sodium atoms. Sodium vapor was produced in an oven and was detected by resonant fluorescence. Since the sodium atoms are lost at the walls with near unit efficiency, the data analysis is quite similar to that of an ion-neutral flow tube reactor (flowing afterglow). In this paper we describe the apparatus which has been developed to study the kinetics and diffusion of Na and Na compounds and present our first work.

II. EXPERIMENTAL

Figure 1 is a diagram of the essential features of the experiment. The flow tube is a 5.08 cm i.d. by 69 cm long copper pipe. Brass flanges with O ring seals are soldered on each end of the flow tube. The downstream flange mates with a conflat flange on a commercial six-way cross. A 1 cm thick Teflon spacer is inserted between the flow tube and the six-way cross to provide thermal insulation. The upstream flange has a 3/4 in. i.d. fitting with an O ring seal in the center for the sodium inlet and a 1/4 in. i.d. fitting with an O ring seal located at the bottom edge of the flow tube wall for the reactant inlet. This arrangement allows the inlets to be moved independently. The carrier gas is introduced through 1/4 in. stainless steel tubing soldered to the upstream flange. Additional reactants can be added to the carrier gas through a tee located upstream of the flow tube. The pressure measurement port is a 1/4 in. copper tube soldered in the approximate center of the reaction zone, 26 cm from the downstream flange of the flow tube. The port is flush with the inside surface of the flow tube to ensure that the true static pressure is measured. The reactor is pumped by a 500 ℓs^{-1} vacuum booster backed by a 66 ℓs^{-1} fore pump. Approximately 75 turns of 1/4 in. copper tubing through which a fluid from a temperature regulated bath is circulated are wrapped around the flow tube to provide temperature variability of the reactor.

Figure 2 is a diagram of the sodium oven. It is constructed from a 2.8 cm o.d. by 3 cm tall cylindrical copper block. Sodium metal is placed in a 1.3 cm i.d. well drilled in the block. A removable copper heat shield rests on top of the well to inhibit upward diffusion of sodium. The copper block is silver soldered to a stainless steel conflat miniflange. A second miniflange serves as the cover for the oven, and with a heat resistant copper gasket, provides a vacuum seal. The oven is heated by several turns of 1.1 mm o.d. coaxially shielded nichrome wire with its inconel sheath soldered directly to the outside of the oven block. The oven temperature is regulated to $\pm$ 0.1 °C by a homemade electronic servo. A chromel alumel thermocouple inserted into a small blind hole in the oven block measures the temperature. This temperature was determined to agree with the temperature of the liquid sodium to within 1 °C. Sodium melts at 370 K and a typical oven temperature was 400 K. A small, $\sim$1 STP $cm^3 s^{-1}$ (STP = 1 atm, 273 K), flow of an inert flush gas carries the sodium vapor into the sodium inlet.

The innermost tube of the sodium inlet is a 100 cm

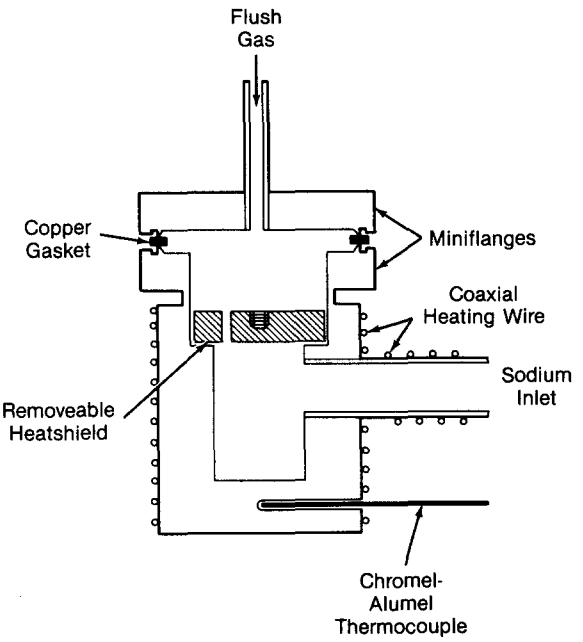

FIG. 2. Sodium oven.

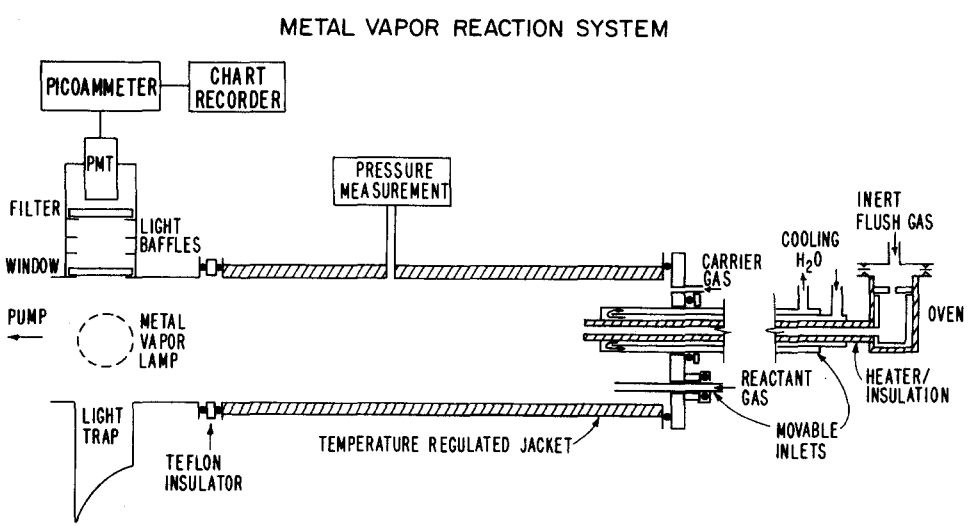

FIG. 1. Sodium flow tube with oven source and resonant fluorescence detection.

length of 3/16 in. o.d. copper tubing. A 200 cm length of coaxially shielded heating wire is silver soldered to the outside of this tubing. A chromel alumel thermocouple is soldered to the tubing 18 cm from the outlet of the injector. The copper tubing and heating wires are wrapped with three layers of 1/16 in. thick glass cloth insulation and inserted into a 1/2 in. o.d. stainless steel cooling jacket. The same fluid used to control the temperature of the flow tube is circulated through the sodium inlet cooling jacket to avoid temperature gradients in the flow tube. Only the heated tip of the sodium inlet and the small flow of oven flush gas, which is $<4\%$ of the total flow, carry heat into the flow tube. The inlet temperature, typically about 500 K, is controlled by a variac. The temperature inside the inlet was measured with a thermocouple probe and was found to vary by less than 10 °C from the outlet to the oven.

The sodium inlet is maintained 60 to 90 °C hotter than the oven to inhibit condensation of Na vapor and to decrease the proportion of Na dimers. Under typical experimental conditions, $T_{oven} = 400$ K and $T_{inlet} = 490$ K, the concentration of Na at the tip of inlet is 2×10^9 atom cm^{-3} and the ratio of sodium dimers to sodium atoms is about 1×10^{-3}. At this level, the Na dimers cannot have a significant effect on the reactions studied here. Only Na_2 reactions that produce Na can perturb the measurements. These reactions involve atoms such as O or Cl which are present only at very low concentrations in these experiments. An experiment that examined possible effects from Na dimers is described in Sec. V.

Sodium is detected by resonant fluorescence at 590 nm using the D line transition. The light source is a low pressure sodium lamp operated at reduced voltage to minimize self-reversal of the D line emission. The light passes through a 6.5 mm aperture and several baffles and into the center of the detection region. A photodiode located across from the light source measures the lamp intensity. Sodium fluorescence is collected at a right angle to the excitation beam through another set of baffles, a suprasil window, and a narrow ($\lambda_{center} = 589$ nm, FWHM = 1 nm, transmission = 30%) bandpass filter. A light trap opposite the phototube minimizes scattered light. The fluorescence signal is detected by a phototube, which is cooled to -30 °C and biased at 1000 V. Both the phototube and photodiode currents are monitored by picoammeters and displayed on a two-pen chart recorder. Since the absorption cross section of sodium atoms is large[35] (1.85×10^5 Å^2), absorption of the D line radiation across the six-way cross and fluorescence can be measured simultaneously for Na concentrations greater than 1×10^8 atom cm^{-3}. In this way the detection limit for resonant fluorescence detection can be calibrated. It is approximately 1×10^4 atom cm^{-3}. This low detection limit allows us to use Na concentrations of 10^4 to 10^8 atom cm^{-3} in the flow tube. Thus we avoid possible problems of self-absorption of the Na fluorescence and eliminate secondary chemistry from reactions between sodium species.

A 10 Torr full-scale differential capacitance manometer measures the pressure in the flow tube. The manometer is calibrated to $\pm$ 1.0% from 0.2 to 7 Torr by comparison with a precision water manometer. Gas flows are measured with mass flow meters which are recalibrated for each gas. Large flows (>15 STP cm^3 s^{-1}) are calibrated to $\pm$ 2% using a wet test meter while small flows (<15 STP cm^3 s^{-1}) are calibrated to the same accuracy by measuring the rate of pressure change in a calibrated volume. The flow of the He/Cl_2 mixture is measured by diverting the flow into calibrated volume immediately after each experiment and measuring the pressure change as a function of time. The uncertainties given are an estimate of the long term accuracy of the manometer and mass flow meters as determined by frequent recalibrations; the accuracy during the calibration is somewhat better, being $\pm$ 0.3% for the manometer and $\pm$ 1.5% for the flowmeters.

The helium (99.9%) and argon (99.999%) are purified by a zeolite trap (50% 5X, 50% 13X molecular sieve) at 78 and 213 K, respectively. The effects of impurities in the carrier gas are discussed in Sec. VI and are shown to be very small. The SF_6 (99.99%) was used as is. The Na metal (analyzed grade, 99.999%) is cut and loaded into the oven in ambient air. This technique worked as well as loading the oven under an argon atmosphere in a glove bag.

A custom mixed cylinder of Cl_2 and He is used as the Cl_2 source. The mole fraction of Cl_2 in the He/Cl_2 mixture is measured optically in a 10 cm absorption cell at the 313 nm Hg line. A plot of the absorption of pure Cl_2 at 11 pressures from 4 to 48 Torr vs pressure gives a Cl_2 absorption cross section at 313 nm of $(2.06\pm0.06)\times10^{-19}$ cm^2, which is in good agreement with the work of Burkholder and Bair[36] who obtained 2.04×10^{-19} cm^2. A plot of the absorption of the mixture at 12 pressures from 22 to 550 Torr vs pressure yields a Cl_2 mole fraction of (6.52 ± 0.15)%. We used our value of the cross section to compute the Cl_2 mole fraction in the mixture, since we feel the systematic errors in both measurements will tend to cancel and our value is not significantly different than the published value. The mole fraction of Cl_2 is somewhat lower than the value of 7.34% that is claimed by the supplier.

III. DATA ANALYSIS

The continuity equation for a species A suffering both a first order chemical reaction loss and a first order wall loss in an axially symmetric cylindrical reactor under laminar flow conditions is[40]

$$2v\left(1-\frac{r^2}{a^2}\right)\frac{\partial A(r,z)}{\partial z} = \left[D\left(\frac{1}{r}\frac{\partial}{\partial r}r\frac{\partial}{\partial r}\right)+D\left(\frac{\partial^2}{\partial z^2}\right)-k_1\right]A(r,z)\,, \qquad (9)$$

where z = axial coordinate, r = radial coordinate, $r=0$ at center of tube, a = tube radius, $A(r,z)$ = concentration of species A at (r,z), k_I = first-order rate constant for chemical reaction = k_{II} [reactant] or k_{III} [reactant] [M], where k_{II} and k_{III} are the bimolecular and termolecular rate coefficients, D = diffusion coefficient of A in carrier gas, and v = average flow velocity. Subject to the boundary condition:

$$D\left.\frac{\partial A(r,z)}{\partial r}\right|_{r=a} = \frac{\gamma c A(r,z)}{2a(1-\gamma/2)}\,, \qquad (10)$$

where γ = sticking probability for species A on the wall and c = mean molecular speed of A. Equation (9) cannot be separated and solved in closed form. More importantly, in general there is not a simple linear relationship between the observed decay of A and the rates of wall loss and chemical reaction.

Fortunately, in many experimental cases approximate solutions can be used with reasonable ($\sim 10\%$) accuracy. In a radical flow tube with $\gamma \ll 1$ the plug flow continuity equation, Eq. (11), can be used:

$$v\frac{\partial A(z)}{\partial z} = \left(k_{\rm I} + D\frac{\partial^2}{\partial z^2}\right)A(z)\ . \tag{11}$$

This is obtained from Eq. (9) by setting the $\partial/\partial r$ terms equal to zero, i.e., assuming there are no radial concentration gradients. In an actual experiment the concentration of A is observed as a function of z and an observed plug flow first order rate constant is derived from a plot of $\ln A(z)$ vs z:

$$k_{\rm obs} = -v\frac{\partial \ln A(z)}{\partial z}\ . \tag{12}$$

A solution to Eq. (11), ignoring loss at the walls but including axial diffusion, is Eq. (13):[37]

$$k_{\rm I} = \left(1 + \frac{k_{\rm obs}D}{v^2}\right)k_{\rm obs}\ . \tag{13}$$

This solution is not valid when γ approaches 1, since the radial profile can no longer be assumed to be uniform. Huggins and Cahn[38] obtained an approximate solution to the laminar flow continuity equation by ignoring axial diffusion and assuming $\gamma = 1$ and wall loss$\gg$reaction loss. These conditions are often found in ion-neutral flow reactors and are close to the conditions found in this work. They assumed a solution of the form $A(r,z) = g(r)\exp(-k_{\rm obs}zv^{-1})$, where $g(r)$ is a two-term expansion in even powers of r. Their solution is Eq. (14):

$$k_{\rm obs} = \frac{7.34\,D}{2a^2} + \frac{1.26k_{\rm I}}{2}\ . \tag{14}$$

For the reaction rate coefficient, this result is identical to the plug flow solution (ignoring axial diffusion) with a correction factor of 2/1.26 or 1.59. Under conditions where the diffusion coefficient does not change between observations, $k_{\rm II}$ is obtained by plotting $k_{\rm obs}$ vs [reactant] and multiplying the slope by 1.59. When there is no reactant, $k_{\rm I} = 0$ and the first order wall loss is linearly related to the diffusion coefficient

$$D = \frac{2a^2}{7.34}k_{\rm obs}\ . \tag{15}$$

The full laminar flow continuity equation can be solved directly by numerical methods. This was first done by Walker.[39] His work has been incorporated into a convenient computer program by Brown.[40] His program, given two of the three variables, $k_{\rm obs}$, $k_{\rm I}$, or D, solves for the third. The program uses a 30-term expansion in even powers of r for the radial profile and treats axial diffusion directly. Silver,[44] using a modified version of Brown's program, has shown that the observed first order rate constant for diffusion limited wall loss is relatively insensitive to the value of the sticking coefficient over the range $0.1 < \gamma < 1$ for cases in which $D < 0.08av$. A plot of D vs p^{-1} will only be linear for large D when $\gamma \approx 1$. This can be used to estimate γ and will be discussed in a future paper.[43] The slope of the D vs p^{-1} plot is D_p, the diffusion coefficient at the reference pressure. In this paper, D_p has units of cm^2 Torr s^{-1}. The rigorous treatment of the data produces results that are generally within 5% of those obtained from the simple relation of Huggins and Cahn.[38]

For an individual measurement of the first order wall loss, the diffusion coefficient, D, in units of cm^2 s^{-1} can be obtained from Eq. (15). Since $v = F_T\,(760/p)\,(T/273)\,(1/\pi a^2)$, where F_T is the total flow in the tube in STP cm^3 s^{-1}, p is the pressure in Torr, and T is in K, D in terms of the experimentally observed quantities is Eq. (16):

$$D = 0.2415F_T T\frac{d\ln A(z)}{dz}\ , \tag{16}$$

where z is measured in cm and D is in cm^2 s^{-1}.

A standard propagation of errors treatment[41] using $(\Delta F_T/F_T) = 0.02$, $(\Delta T/T) = 0.01$, and $(\Delta_{\rm slope}/{\rm slope}) = 0.03$, where slope $= d\ln A(z)/dz$, yields a diffusion coefficient precision of 4.0% at the 95% confidence level. Note that the precision of the individual measurements does not depend on the pressure or the tube dimensions. The advantage of measuring the diffusion coefficient over a large pressure range is that it checks for systematic errors such as carrier gas impurities or breakdown of the assumption that $\gamma \approx 1$. These errors are included in the overall uncertainty. The measurement precision for the second order rate constant is necessarily poorer than that of the diffusion coefficient, since more experimental quantities must be accurately measured. A calculation similar to our previous work[42] gives a precision of 7.5% for the second order rate constant. Possible systematic errors are similar to those in the diffusion coefficient and are discussed in Sec. VI. The diffusion coefficients are reported with a 10% uncertainty and the rate constants are reported with a 20% uncertainty, both at the 95% confidence level.

IV. DIFFUSION COEFFICIENTS

Measurements of the first order-wall loss rate constant were made by observing the sodium resonant fluorescence signal as a function of Na inlet position. The decay plots were very linear as can be seen in Fig. 4 for the $[Cl_2] = 0.0$ experiment. The flow tube pressure was varied from 0.17 to 4.8 Torr, and covered a range of at least a factor of 20 for each gas. Flow velocities ranged from 400 to 9500 cm s^{-1}. Each wall loss measurement was converted to a diffusion coefficient using Brown's program[40] and assuming $\gamma = 1$. As discussed in Sec. III this method accounts for axial diffusion. We have shown that γ lies between 0.3 and 1 for our flow tube and that the value of the diffusion coefficient is insensitive to the exact value of γ in that range.[43] Brown's analysis[40] gave diffusion coefficients that were generally within 3% of those obtained from the simple analysis of Huggins and Cahn,[38] Eq. (15), although some of the low pressure measurements in He ($D \approx 1750$ cm^2 s^{-1}) had differences of up to 6.5%. D vs p^{-1} plots for He and Ar are shown in Fig. 3 and the tabulated results are shown in Table I. The intercepts of

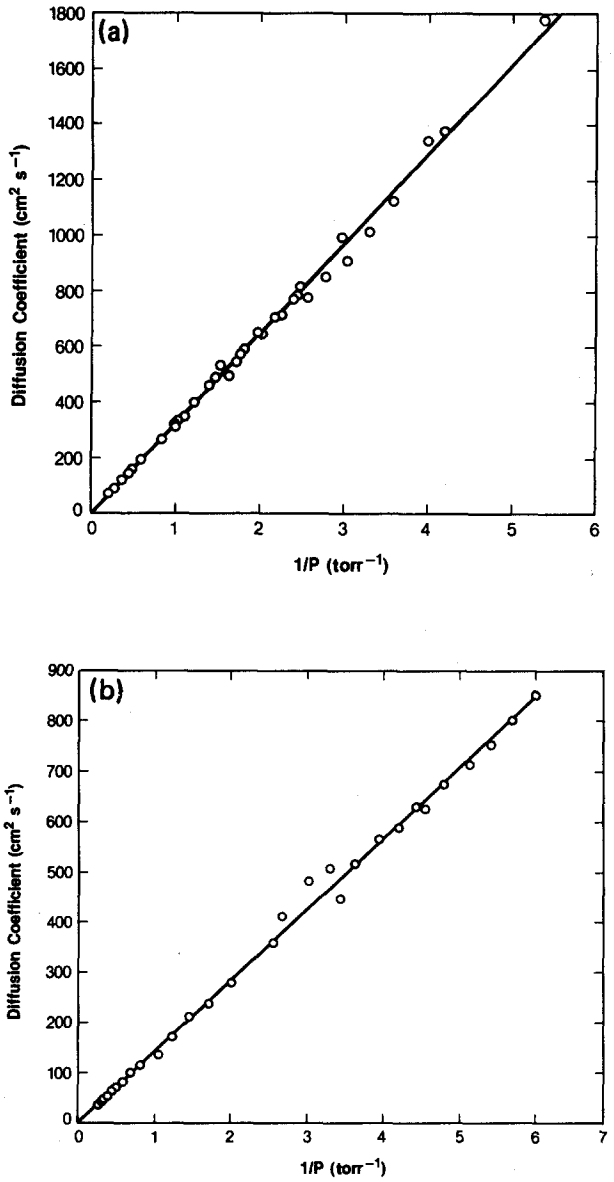

FIG. 3. D vs p^{-1} plots, D obtained by method of Brown (see the text): (a) 36 measurements of k_I, carrier gas is He, $T = 290$ K, the slope $= D_p = 325 \pm 33$ cm^2 Torr s^{-1}; (b) 29 measurements of k_I carrier gas is Ar, $T = 281$ K, the slope $= D_p = 140 \pm 14$ cm^2 Torr s^{-1}.

these plots are not significantly different than zero. The slope of the D vs p^{-1} plot is the reported diffusion coefficient. $D_{Na,He} = (325 \pm 33)$ cm^2 Torr s^{-1} at 290 K and $D_{Na,Ar} = (140 \pm 14)$ cm^2 Torr s^{-1} at 281 K.

V. Na ATOM KINETICS

As a test of the apparatus the rate coefficients of reactions (17) and (18) were measured:

TABLE I. Summary of measured diffusion coefficients.

Carrier gas	T (K)	No. of expts.	p range (Torr)	D^a (cm^2 Torr s^{-1})
He	290	36	0.186–4.78	325 ± 33
Ar	281	29	0.167–3.67	140 ± 14

[a] Obtained from k_{obs} by the method of Brown as described in the text.

$$Na + Cl_2 \rightarrow NaCl + Cl, \quad \Delta H^0_{298} = -40.3 \text{ kcal mol}^{-1}, \tag{17}$$

$$Na + SF_6 \rightarrow NaF + SF_5, \quad \Delta H^0_{298} = -21.4 \text{ kcal mol}^{-1}. \tag{18}$$

No products were observed so the reactions are written as we believe they proceed. Reaction (17) allows us to check for possible effects from Na dimers in the flow tube, since reaction (19) is known to be chemiluminescent, producing D line emission[23]

$$Cl + Na_2 \rightarrow NaCl + Na(^2P). \tag{19}$$

No D line chemiluminescence was observed at [Na] of up to about 1×10^9 atom cm^{-3} at the tip of the sodium inlet and [Cl_2] of up to 1×10^{13} molecule cm^{-3}. Therefore the D line signal under our experimental conditions comes wholly from the fluorescence of Na atoms excited by the lamp and the concentration of Na dimers is sufficiently small as to not perturb the measurements. This test also demonstrates the absence of significant secondary chemistry as expected for the low concentrations used in our experiment.

For the rate measurements, the reactant gas inlet was fixed 5 cm from the upstream flange, assuring a unform radial distribution of the reactant in the reaction zone. As with the diffusion coefficient measurements, the resonant fluorescence signal was recorded as a function of Na inlet position to measure a first order rate constant. The approximate solution to the continuity equation given in Eq. (14) shows that k_{obs} will be a function of the diffusion coefficient and thus of pressure. Therefore, the pressure and velocity were held constant for a set of runs while the concentration of the reactant $(1\text{–}20) \times 10^{11}$ molecule cm^{-3} for Cl_2 and $(2\text{–}30) \times 10^{13}$ molecule cm^{-3} for SF_6, was varied.

For Na + Cl_2, 54 measurements of k_{obs} were performed at eight different pressures and velocities ranging from 0.260

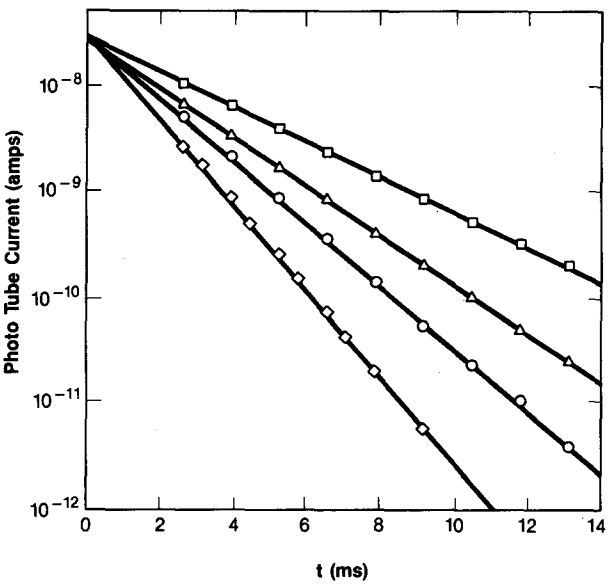

FIG. 4. Sample decay plots for Na + Cl_2: $v = 3780$ cm s^{-1}, $p = 0.538$ Torr; (□) [Cl_2] = 0; (△) [Cl_2] = 3.03×10^{11} molecule cm^{-3}; (○) [Cl_2] = 6.12×10^{11} molecule cm^{-3}; (◇) [Cl_2] = 1.12×10^{12} molecule cm^{-3}.

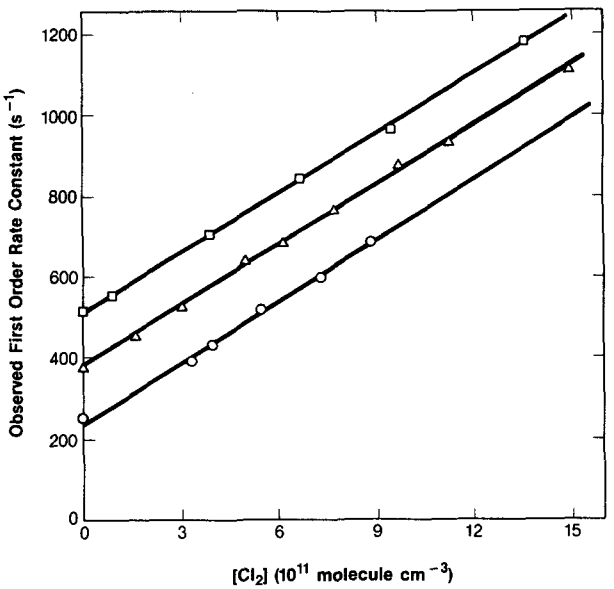

FIG. 5. Sample k_{obs} vs $[Cl_2]$ plots: (□) $p = 0.395$ Torr; (△) $p = 0.538$ Torr; (○) $p = 0.806$ Torr; $k_{II} = (7.80 \pm 1.6) \times 10^{-10}$ cm^3 $molecule^{-1}$ s^{-1}.

from 0.260 to 1.37 Torr and 1500 to 8400 cm s^{-1}. Sample decay plots are shown in Fig. 4. Typical k_{obs} vs $[Cl_2]$ plots are shown in Fig. 5 for three different pressures and velocities. The intercepts of these plots are the first order wall loss rate constants and are proportional, as expected, to p^{-1}. Each k_{obs} was converted to a k_I by the method of Brown.[40] This method accounts for the effects of axial diffusion and radial concentration profile. This k_I was plotted vs $[Cl_2]$, the slope being the second order rate coefficient. In Sec. VI, this treatment is compared to that of Huggins and Cahn.[38] The results of both treatments are reported in Table II. The rate constant for Na + Cl_2 at 293 K is $(7.80 \pm 1.6) \times 10^{-10}$ cm^3 $molecule^{-1}$ s^{-1}.

Twenty-eight measurements of k_{obs} for Na + SF_6 were made at four pressures and in two carrier gases, He and CO_2, at 281 K. The pressure ranged from 0.4 to 1.4 Torr and the velocity from 850 to 2500 cm s^{-1}. The results for the second order rate constant are shown in Table III. The rate constant for Na + SF_6 is $(1.17 \pm 0.2) \times 10^{-12}$ cm^3 $molecule^{-1}$ s^{-1}.

VI. DISCUSSION

Measuring the diffusion coefficient over a large pressure range allows us to check for systematic errors. The near zero intercepts of the D vs p^{-1} plots (Fig. 3) show that the observed first order Na loss is due only to diffusion controlled wall removal. A reactive impurity in the carrier gas leads to a functional dependence of the form, $k_{obs} = aDp^{-1} + bp$, which yields positive intercept in the limit of $p^{-1} \rightarrow 0$. Failure to observe such intercepts proves that the contribution from gas phase reactions with carrier gas impurities is completely negligible.

Table IV is a comparison of this work to selected previous measurements of $D_{Na,He}$[24,31,44–47,49] and $D_{Na,Ar}$.[24,44,45,47] Note that this work covers a larger pressure range than all previous experiments. Agreement is very good with Silver[44] who performed a similar experiment in a larger diameter tube (7.26 cm) and who also used the analysis of Brown.[40] Agreement is fairly good with the other experiments, except the flash photolysis-resonant absorption work of Husain and Plane.[31] However, the diffusion coefficients at 724 and 844 K for Na in He reported in that work imply a temperature dependence of $T^{-7.8}$. This is clearly nonphysical as experimental results on many gaseous systems[48] show that the temperature dependence is usually very close to $T^{1.7}$. For this reason a $T^{1.7}$ dependence was used to extrapolate the various experimental results to 300 K for comparison in Table IV. Agreement with Redko[50,51] who used theoretically calculated potentials[52–54] in his Chapman–Enskog calculations is fairly good. More recently, the Na–He,[55] Na–Ne,[56] and Na–Ar[57] potentials have been reinvestigated by spectroscopic methods. Calculations based on these potentials are in reasonable agreement with our experimental diffusion coefficients and will be reported later.[43]

Table II compares the results of the simple analysis of Huggins and Cahn[38] with the more rigorous treatment of Brown[40] for the Na + Cl_2 rate constant measurements. The differences between the two treatments are small. The maximum difference between the two treatments is 8.2% and the average difference is 6.1%. If the difference is due primarily to the effects of axial diffusion, which the simple treatment assumes to be small, one can see from Eq. (13) that the difference would be greatest for large k_{obs} and slow velocity. This is indeed the case with these measurements with the

TABLE II. Na + Cl_2 kinetic measurements.

p (Torr)	No. of expts.	T (K)	v (cm s^{-1})	$[Cl_2]$ (10^{11} molecule cm^{-3})	k_{II}^a (10^{-10} cm^3 $molecule^{-1}$ s^{-1})	k_{II}^b (10^{-10} cm^3 $molecule^{-1}$ s^{-1})
0.260	6	292	8400	2.7–14	7.16	7.35
0.303	9	293	6360	0.86–20	7.45	7.77
0.395	6	293	4200	0.91–14	7.91	8.38
0.538	9	293	3780	1.6–15	7.97	8.44
0.640	6	292	2300	3.6–14	6.16	6.65
0.806	6	293	1930	3.3–8.8	7.97	8.62
1.05	6	293	2170	2.5–13	7.51	8.04
1.37	6	293	1500	3.0–9.9	6.69	7.18
					Recommended value	7.80 ± 1.6

[a] Obtained from k_{obs} by the method of Huggins and Cahn as described in the text.
[b] Obtained from k_{obs} by the method of Brown as described in the text.

TABLE III. Na + SF_6 kinetic measurements at 281 K.

Carrier gas	p (Torr)	No. of expts.	$[SF_6]$ (10^{13} molecule cm^{-3})	k_{II}^a (10^{-12} cm^3 molecule^{-1} s^{-1})
CO_2	0.395	8	1.8–11	1.04
CO_2	0.570	8	3.1–15	1.33
CO_2	1.37	6	6.8–30	1.20
He	0.939	6	2.6–11	1.07
			Recommended value	1.17 ± 0.2

[a] Obtained from k_{obs} by the method of Brown as described in the text.

largest differences coming from the sets with the slowest velocities.

The Na + SF_6 reaction exhibits second order kinetics as demonstrated by consistent results with He and CO_2 as buffer gases and lack of a measurable pressure effect over the small pressure range, 0.4 to 1.4 Torr. SF_5 and NaF are assumed to be the products, as no other exothermic paths are obvious. Since the reaction rate constant is small compared to the expected collision rate, the possibility that the observed reaction was due to impurities in the SF_6 was considered. Assuming a rate constant of 5×10^{-10} cm^3 molecule^{-1} s^{-1} for the impurity reaction with Na, the reactive impurity would have to be 0.02% of the SF_6 to raise the rate constant by 10%. At an impurity level of 0.01%, the maximum indicated by the manufacturer, the effective rate constant would only be 5×10^{-14}, which is less than 5% of the measured value. Moreover, the major impurities in the SF_6 are O_2, N_2, and H_2O, none of which have an exothermic second order gas phase reaction with Na. Therefore, the observed Na decay is most certainly due to reaction with SF_6.

Table V compares our result for the Na + Cl_2 rate constant with three previous studies. Our result is in good agreement with the recent work of Silver[67] who obtained $(6.7 \pm 0.9)\times10^{-10}$ cm^3 molecule^{-1} s^{-1} using a similar technique. Maya and Davidovits[58] used a flash photolysis-resonant absorption technique and obtained $(1.38 \pm 0.2)\times10^{-9}$ cm^3 molecule^{-1} s^{-1} at 1015 K. Their rate constant extrapolated to 300 K using a $T^{0.5}$ temperature dependence is $(7.5 \pm 1.1)\times10^{-10}$ cm^3 molecule^{-1} s^{-1} which is in good agreement with this work. Polanyi,[23] using a diffusion flame technique, measured 6.8×10^{-10} cm^3 molecule^{-1} s^{-1} at ~600 K. This extrapolates to 4.8×10^{-10} cm^3 molecule^{-1} s^{-1} at 300 K, which is in fairly good agreement with this work. Polanyi[23] observed evidence of reaction (19) which reforms Na and may have caused an underestimate of the rate constant. The present result is ~40% lower than a value we reported earlier.[69] The Na + Cl_2 experiments were repeated because of the large discrepancy with the result of Silver[67] and because it was suggested that the mass flowmeter used in the earlier study may give erroneous results. Unfortunately, the exact source of error in the previous study cannot be identified because the mass flowmeter has been recalibrated for other gases in the meantime and the original He/Cl_2 mixture is no longer available.

Husain and Marshall[59] have published the only other measurement of the Na + SF_6 rate constant. Their flash photolysis-resonant absorption technique gave $(5.5 \pm 1.2)\times10^{-10}\exp(-1240 \pm 145/T)$ cm^3 molecule^{-1} s^{-1} over the temperature range 644–918 K. This extrapolates to a value of 7.7×10^{-12} cm^3 molecule^{-1} at 290 K, which is a factor of 7 higher than our measurements. We do not have an explanation for this poor agreement. Forcing the Arrhenius fit through our rate constant results in the expression $k(T)\approx6.4\times10^{-10}\exp(-1770/T)$ cm^3 molecule^{-1} s^{-1},

TABLE IV. Summary of measured diffusion coefficient for Na in He and Ar.

Reference	Method[a]	T range (K)	p range (Torr)	$D^b_{Na,He}$ (cm^2 Torr s^{-1})	$D^b_{Na,Ar}$ (cm^2 Torr s^{-1})
This work	oven source, flow tube, RF	280–290	0.17–4.8	345 ± 35	160 ± 16
Silver (Ref. 44)	oven source, flow tube, LIF	He:309–473 Ar:322–350	1–8	360 ± 50	160 ± 75
Husain and Plane (Ref. 31)[c]	flash photolysis-resonant absorption	724,844	15–100	630,190	
Fairbank *et al.* (Ref. 45)[d]	transit time of single atom across laser beam	315	100–400	360	200
Bichi *et al.* (Ref. 46)	spin relaxation	453	200	440 ± 60	
Kumuda *et al.* (Ref. 47)	Stefan method	653–833	760	360 ± 40	150 ± 15
Ramsey and Anderson (Ref. 49)	spin relaxation	428	80–990	370	
Hartel *et al.* (Ref. 24)	diffusion flame	655	1.4	420	180
Redko (Refs. 50 and 51)	Chapman–Enskog calculations using model potentials	300–3000		380	135

[a] RF, resonant fluorescent; LIF, laser induced fluorescence.
[b] Extrapolated to 300 K using a temperature dependence of $T^{1.7}$; error limits are those of the authors, if reported.
[c] Values are as reported for each temperature, extrapolations are those of the authors who used $T^{1.5}$.
[d] Average of the two reported values.

TABLE V. Summary of measured rate constants for Na + Cl_2.

Reference	Method[a]	T (K)	k_{II} (cm^3 $molecule^{-1}$ s^{-1})
This work	oven source, flow tube, RF	293	$(7.80 \pm 1.6) \times 10^{-10}$
Silver (Ref. 67)	oven source, flow tube, LIF	294	$(6.7 \pm 0.9) \times 10^{-10}$
Maya and Davidovits (Ref. 58)	flash photolysis-resonant absorption	1015	$(1.38 \pm 0.2) \times 10^{-9}$
Polanyi (Ref. 23)	diffusion flame	600	6.8×10^{-10}

[a] RF, resonant fluorescence; LIF, laser induced fluorescence.

which has a somewhat larger activation energy than that given by the data of Husain and Marshall[59] alone.

The electron jump model[28] calculates the distance at which it is thermoneutral for an electron to jump from the alkali metal to the reactant. This leads to the expression, $r_{jump} = 14.35/(\text{I.P.-E.A.})$,[60] where r is the separation in Å and the ionization potential and the electron affinity are in eV. The model has had considerable success in qualitatively predicting the large cross sections for reaction and forward scattering of alkali metal + halogen molecule interactions studied in molecular beams and diffusion flames. A rate constant is calculated as $k = \pi r_{jump}^2 v_{rel}$, where v_{rel} is the average relative velocity of the reacting pair. The model predicts 5.1×10^{-10} cm^3 $molecule^{-1}$ s^{-1} at 300 K for the rate constant of Na + Cl_2 using I.P.(Na) = 5.138 eV[61] and E.A. (Cl_2) = 2.38 eV.[62] A hard-sphere model using $r_{Na} = 2.45$ Å calculated from our $D_{Na,He}$ measurement and $r_{Cl_2} = 2.71$ Å calculated from the Cl_2 viscosity[64] of 1.33×10^{-4} P at 293 K also yields 5.0×10^{-10} cm^3 $molecule^{-1}$ s^{-1} as the collision rate constant. We are surprised that the hard-sphere value is as large as the electron jump value. Our measured rate constant exceeds the predictions of both models by a factor of 1.5. Davidovits and co-workers[63] have measured the rate constants of all the combinations of Li, Na, K, Rb, and Cs with Cl_2, Br_2, and I_2. Using recently measured values for the electron affinities of Cl_2,[62] Br_2,[62] and I_2,[65] the only other alkali metal–halogen reaction whose measured rate constant exceeds the prediction of the electron jump model is Na + Br_2. The measured rate constant for that reaction exceeds the electron jump model prediction by a factor of 1.3. These experimental results show that the simple electron jump model is not a strict upper limit for alkali metal–halogen molecule reaction rate constants. Gislason[68] has proposed a "refined" electron jump model that includes an attractive potential of the form $V(R) = -C_0 R^{-6}$. This increases the electron jump rate constant and predicts 8.4×10^{-10} cm^3 $molecule^{-1}$ s^{-1} for the rate constant of Na + Cl_2, which is a much better agreement with the experimental data.

Using E.A.(SF_6) = 1.05 eV,[66] the electron jump model predicts 2.21×10^{-10} cm^3 $molecule^{-1}$ s^{-1} for the Na + SF_6 rate constant at 300 K. In this case, the measured rate constant is nearly 200 times smaller. Although an electron jump mechanism may provide a long range attraction, it is clear that not every collision is reactive. This reaction probably proceeds by a rebound mechanism,[29] in analogy with Na + CH_3I. These reactions have smaller reaction cross sections and less forward scattering than the electron jump reactions.[29]

Further studies with this experiment are in progress on the temperature dependence of Na diffusion coefficients and on the reactions of Na and NaO with various atmospheric gases and organic compounds.

ACKNOWLEDGMENT

This work was supported in part by the Chemical Manufacturers Association Technical Panel on Fluorocarbon Research.

[1] V. M. Slipher, Publ. Astron. Soc. Pac. **41**, 263 (1929).
[2] J. Cabannes, J. Dufay, and J. Gauzit, Astrophys. J. **88**, 164 (1938).
[3] S. Chapman, Astrophys. J. **90**, 309 (1939).
[4] B. W. Currie and H. W. Edwards, Terr. Magn. Atmos. Electron. **41**, 265 (1936).
[5] R. Bernard, Astrophys. J. **89**, 133 (1939).
[6] V. W. J. H. Kirchhoff and B. R. Clemensha, J. Atmos. Terr. Phys. **35**, 1493 (1973).
[7] G. Megie and J. E. Blamont, Planet. Space Sci. **25**, 1093 (1977).
[8] G. Megie, F. Bos, J. E. Blamont, and M. L. Chanin, Planet. Space Sci. **26**, 27 (1977).
[9] D. M. Hunten and L. Wallace, J. Geophys. Res. **72**, 69 (1967).
[10] T. M. Donahue and R. R. Meier, J. Geophys. Res. **72**, 2803 (1967).
[11] J. E. Blamont and T. M. Donahue, J. Geophys. Res. **66**, 1407 (1961).
[12] B. R. Clemesha, V. W. J. H. Kirchhoff, D. M. Simonich, and H. Takahashi, Geophys. Res. Lett. **5**, 873 (1978).
[13] C. E. Junge, O. Oldenberg, and J. T. Wasson, J. Geophys. Res. **67**, 1027 (1962).
[14] E. E. Ferguson, Geophys. Res. Lett. **5**, 1035 (1978).
[15] F. Arnold, D. Krankowsky, and K. H. Marien, Nature (London) **267**, 30 (1977).
[16] F. Arnold, H. Böhringer, and G. Henschen, Geophys. Res. Lett. **5**, 653 (1978).
[17] S. C. Liu and G. C. Reid, Geophys. Res. Lett. **6**, 283 (1979).
[18] E. Murad, W. Swider, and S. W. Benson, Nature (London) **289**, 273 (1981).
[19] F. S. Rowland and P. J. Rogers, Proc. Natl. Acad. Sci. U.S.A. **79**, 2737 (1980).
[20] J. J. Lamb and S. W. Benson, J. Geophys. Res. (in press).
[21] E. Arijs, D. Nevejans, and J. Ingels, Nature (London) **288**, 684 (1980).
[22] F. Arnold, G. Henschen, and E. E. Ferguson, Planet. Space Sci. **29**, 185 (1981).
[23] M. Polanyi, *Atomic Reactions* (Williams and Norgate, London, 1932).
[24] H. Hartel, N. Meer, and M. Polanyi, Z. Phys. Chem. (Leipzig) **199**, 139 (1932).
[25] F. Haber and H. Sachsse, Z. Phys. Chem. Bodenstein–Festband **1931**, 831.
[26] W. Heller and M. Polanyi, Trans. Faraday Soc. **32**, 633 (1936).
[27] C. E. H. Bawn and A. C. Evans, Trans. Faraday Soc. **33**, 1580 (1937).
[28] J. L. Magee, J. Chem. Phys. **8**, 687 (1940).
[29] J. L. Kinsey, in *MTS International Review of Science, Physical Chemistry Series*, edited by J. C. Polanyi (Butterworths, London, 1972), Vol. 9, pp. 173–212.

[30]A. J. Hynes, M. Steinberg, and K. Schofield, J. Chem. Phys. **80**, 2585 (1984).
[31]D. Husain and J. M. C. Plane, J. Chem. Soc. Faraday Trans. 2 **78**, 163 (1982).
[32]D. Husain, P. Marshall, and J. M. C. Plane, J. Chem. Soc. Faraday Trans. 2 **81**, 301 (1985).
[33]J. A. Silver, M. S. Zahniser, A. C. Stanton, and C. E. Kolb, in *20th Symposium (International) on Combustion* (The Combustion Institute, Pittsburgh, 1984), p. 605.
[34]J. A. Silver, A. C. Stanton, M. S. Zahniser, and C. E. Kolb, J. Phys. Chem. **88**, 3123 (1984).
[35]A. Gaupp, P. Kuske, and H. J. Andrä, Phys. Rev. A **26**, 3351 (1982).
[36]J. B. Burkholder and E. J. Bair, J. Phys. Chem. **87**, 1859 (1983).
[37]F. Kaufman, Prog. React. Kinet. **1**, 3 (1961).
[38]R. W. Huggins and J. H. Cahn, J. Appl. Phys. **38**, 180 (1967).
[39]R. E. Walker, Phys. Fluids **4**, 1211 (1961).
[40]R. L. Brown, J. Res. Natl. Bur. Stand. **83**, 1 (1978).
[41]R. J. Cvetanović, D. L. Singleton, and G. Paraskevopoulos, J. Phys. Chem. **83**, 50 (1979).
[42]C. J. Howard, J. Phys. Chem. **83**, 3 (1979).
[43]J. W. Ager III and C. J. Howard, J. Chem. Phys. (submitted).
[44]J. A. Silver, J. Chem. Phys. **81**, 5125 (1984).
[45]W. M. Fairbank, C. Y. She, and J. V. Prodan, Proc. SPIE Int. Soc. Opt. Eng. **286**, 94 (1981).
[46]P. Bichi, L. Moi, P. Savino, and B. Zambon, Nuovo Cimento B **55**, 1 (1980).
[47]T. Kumuda, R. Ishiguro, and Y. Kimachi, Nucl. Sci. Eng. **70**, 73 (1979).
[48]T. R. Marrero and E. A. Mason, J. Phys. Chem. Ref. Data **1**, 3 (1972), p. 35.
[49]A. T. Ramsey and L. W. Anderson, Nuovo Cimento **32**, 1151 (1964).
[50]T. P. Redko, Opt. Spectrosc. (USSR) **52**, 461 (1982).
[51]T. P. Redko, Sov. Phys. Tech. Phys. **28**, 1065 (1983).
[52]J. Pascale and J. Vandeplanque, J. Chem. Phys. **60**, 2278 (1974).
[53]M. Krauss, P. Maldonado, and A. C. Wahl, J. Chem. Phys. **54**, 4944 (1971).
[54]J. Hanssen, R. McCarroll, and P. Valiron, J. Phys. B **12**, 899 (1971).
[55]M. D. Havey, S. E. Frolking, and J. J. Wright, Phys. Rev. Lett. **45**, 1783 (1980).
[56]R. A. Gottscho, R. Ahmad-Bitar, W. P. Lapatovich, I. Renhorn, and D. E. Pritchard, J. Chem. Phys. **75**, 2546 (1981).
[57]J. Tellinghuisen, A. Ragone, M. S. Kim, D. J. Auerbach, R. E. Smalley, L. Wharton, and D. H. Levy, J. Chem. Phys. **71**, 1283 (1979).
[58]J. Maya and P. Davidovits, J. Chem. Phys. **61**, 1082 (1974).
[59]D. Husain and P. Marshall, J. Chem. Soc. Faraday Trans. 2 **81**, 613 (1985).
[60]R. D. Levine and R. B. Bernstein, *Molecular Reaction Dynamics* (Oxford University, New York, 1974), p. 87.
[61]H. M. Rosenstock, D. Draxl, B. W. Steiner, and J. T. Herron, J. Phys. Chem. Ref. Data **6**, Suppl. 1 (1977).
[62]W. A. Chupka, J. Berkowitz, and D. Gutman, J. Chem. Phys. **55**, 2724 (1971).
[63]P. Davidovits, in *Alkali Halide Vapors*, edited by P. Davidovits and D. L. McFadden (Academic, New York, 1979), pp. 331–344.
[64]*Handbook of Chemistry and Physics*, 56th ed., edited by R. C. Weast (CRC, Cleveland, 1975), p. F-57.
[65]A. P. M. Baede, Physica (Utrecht) **59**, 541 (1972).
[66]E. P. Grimsrud, S. Chowdhury, and P. Kebarle, J. Chem. Phys. **83**, 1059 (1985).
[67]J. A. Silver, J. Chem. Phys. (in press).
[68]E. A. Gislason, in *Alkali Halide Vapors*, edited by P. Davidovits and D. L. McFadden (Academic, New York, 1979), pp. 415–440.
[69]J. W. Ager and C. J. Howard, presented at American Geophysical Union Spring Meeting, Baltimore, Maryland, 1985 and Seventeenth International Symposium on Free Radicals, Granby, Colorado, 1985.